

Photocatalytic Properties of Ordered Double Perovskite Oxides

Hironori Iwakura^{*1}, Hisahiro Einaga^{*2}, Yasutake Teraoka^{*2}

^{*1}Interdisciplinary Graduate School of Engineering Sciences, Kyushu University

^{*2}Faculty of Engineering Sciences, Kyushu University

(Received October 26, 2010; accepted November 25, 2010)

Ordered double perovskite oxides ($A_2BB'O_6$, $AA'BB'O_6$) which contained W, Ta, Nb and Ti were synthesized, and the applicability of the oxides to photocatalytic reaction was discussed. The stability of the oxides strongly depended on the constituent atoms, especially B-site cations. Ta-, Nb- and Ti-containing perovskites were stable under two types of photocatalytic reaction conditions, namely, H_2 evolution from aqueous methanol solution and O_2 evolution in Ag^+ ion-containing aqueous solution. Among the perovskite oxides, La_2ZnTiO_6 showed catalytic activity for the latter reaction and the rate for O_2 evolution normalized by catalyst surface area was one third of that of TiO_2 .

1. Introduction

Photocatalytic reactions over semiconductors have attracted much attention over several decades because they can utilize solar energy for chemical reactions such as overall water splitting^{1,2}). Photocatalytic events in semiconductor are undertaken by absorption of near UV or visible light to generate excited electron-hole pairs, and these species migrate to catalyst surface and result in redox reactions. The charge separation process, one of the most important steps in photocatalytic reaction, strongly depends on the crystal structure and the constituent elements in the catalyst.

So far, many photocatalysts have been developed with different crystal structures, and most of them contain W^{6+} , Ta^{5+} , Nb^{5+} and Ti^{4+} cations because these species are effective in obtaining photocatalytic activities^{1,2}).

Perovskite-type oxide has general formula of $A^{n+}B^{m+}O_3$ ($n + m = 6$), and most of metal cations are known to be stably incorporated in the structure. Perovskite-type oxides are also possible candidates for photocatalytic materials, and several kinds of perovskite-type oxides such as $A^+B^{5+}O_3$ ($A^+ = Ag, Li, Na, K, B^{5+} = Ta, Nb$)^{3,4}) and $A^{2+}In_{0.5}Nb_{0.5}O_3$ ($A^{2+} = Ba, Sr, Ca$)⁵) have been reported to be active for photocatalytic reactions.

Ordered double perovskite ($A_2BB'O_6$, $AA'BB'O_6$) is well known as a subclass of perovskite-type oxide. In the structure, two kinds of metal cations occupy B-site in the same molar ratio, and the metal cations arrange alternately at B-site⁶). The most favorable arrangement is the rock-salt ordering as shown in Fig. 1⁷), and in addition to Ta^{5+} , Nb^{5+} and Ti^{4+} cations, W^{6+} cation is also possible

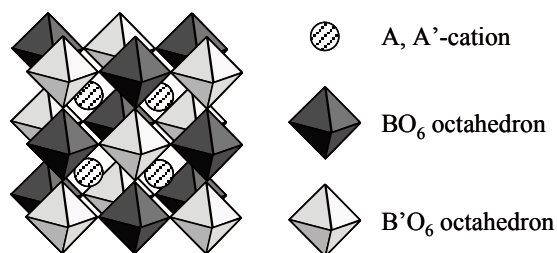


Fig. 1 Crystal structure of ordered double perovskite with rock-salt ordering of B-cations.

to be stably incorporated in ordered double perovskite^{6,8}).

In the present study, ordered double perovskites which contain W^{6+} , Ta^{5+} , Nb^{5+} and Ti^{4+} cations at B-sites have been synthesized and their photocatalytic properties under UV-light irradiation have been investigated. Photocatalytic H_2 production from aqueous methanol solution and O_2 evolution from Ag ion-containing aqueous solution were used to investigate activities of photogenerated electron and hole, respectively. From the results of photocatalytic activity, the applicability of the ordered double perovskites to photocatalytic reactions was discussed from the standpoint of catalyst stability and activity.

2. Experimental

2.1 Preparation and characterization of perovskite oxides

Polycrystalline powders of perovskite-type oxides were synthesized by a conventional solid-state reaction. The starting materials are listed in the footnote of Table 1. The materials were adequately mixed in the stoichiometric ratio by a pestle and mortar and then by a universal ball mill. The mixture was calcined under the conditions which are also shown in Table 1. TiO_2 (JRC-TIO-4, identical to P25, $S_{BET} = 55 \text{ m}^2/\text{g}$) was supplied from Catalysis Society of Japan and used as a reference photocatalyst.

The crystal structures of samples thus prepared were examined by powder XRD measurement using Cu-K α irradiation (Rigaku, RINT-2200) and were refined by Rietveld method using RIETAN-2000 program⁹). The surface area of a sample was determined by BET method from N_2 adsorption isotherm at 77 K (BEL JAPAN, Inc., BELSORP-mini). Diffuse reflectance (DR) UV-VIS spectra of samples were measured using Shimadzu UV-3100 spectrophotometer equipped with an integrating sphere attachment. $\alpha\text{-Al}_2\text{O}_3$ powder was used as a reference sample. The mixture of prepared sample and Al_2O_3 powder was used to obtain a reflectance spectrum, and the spectrum was transformed into the Kubelka-Munk function.

Table 1 Synthesis conditions and crystal structures of ordered double perovskites synthesized in this study

Compound ^{a)}	Calcination condition	Cell parameter (<i>a</i> , <i>b</i> , <i>c</i> / nm, β / °)
Ba ₂ CoWO ₆	1100 °C, 10 h	<i>a</i> = 0.810621(6)
Ba ₂ NiWO ₆	1100 °C, 10 h	<i>a</i> = 0.806676(6)
Ba ₂ CuWO ₆	1000 °C, 5 h	<i>a</i> = 0.55668(3), <i>c</i> = 0.86289(5)
Ba ₂ ZnWO ₆	1100 °C, 10 h	<i>a</i> = 0.812161(6)
Sr ₂ CoWO ₆	1200 °C, 20 h	<i>a</i> = 0.558195(5), <i>c</i> = 0.798172(8)
Sr ₂ NiWO ₆	1100 °C, 5 h	<i>a</i> = 0.555965(4), <i>c</i> = 0.791745(7)
Sr ₂ CuWO ₆	1000 °C, 5 h	<i>a</i> = 0.54283(1), <i>c</i> = 0.84131(2)
Sr ₂ ZnWO ₆	1100 °C, 20 h	<i>a</i> = 0.56321(4), <i>b</i> = 0.56089(3), <i>c</i> = 0.79235(4), β = 89.99(3)
LaBaCoTaO ₆ ^{b)}	1300 °C, 20 h	<i>a</i> = 0.8067(1)
LaBaNiTaO ₆ ^{b)}	1300 °C, 20 h	<i>a</i> = 0.8024(1)
LaBaCoNbO ₆ ^{b)}	1300 °C, 20 h	<i>a</i> = 0.8068(1)
LaBaNiNbO ₆ ^{b)}	1300 °C, 20 h	<i>a</i> = 0.8032(1)
LaBaZnNbO ₆ ^{b)}	1200 °C, 50 h	<i>a</i> = 0.80863(5)
La ₂ ZnTiO ₆	1200 °C, 20 h	<i>a</i> = 0.55746(1), <i>b</i> = 0.56167(1), <i>c</i> = 0.78922(2), β = 90.01(1)

a) Starting material (purity, origin); La₂O₃ (>99.99%, KI), BaCO₃ (>99%, KI), SrCO₃ (>99.9%, KA), Co₃O₄ (>99.9%, KO), NiO (>98%, KI), CuO (>99%, KI), ZnO (>99.5%, KI), WO₃ (>99.9%, KI), Ta₂O₅ (>99.9%, W), Nb₂O₅ (>99.9%, KI), TiO₂ (>98%, KI), Origin: KI; Kishida Chem. Co., Ltd., KA; Kanto Chem. Co., Inc., KO; Kojundo Chem. Lab. Co., Ltd., W; Wako Pure Chem. Industries.

b) Cell parameters were determined from the analysis of PXRD patterns. Those of the other samples were determined by Rietveld refinement.

2.2 Catalyst stability test

Stability of catalyst samples under photoirradiation was investigated in methanol-water solution (50 vol%) and aqueous solution which contained 0.02 M AgNO₃. Catalyst sample (50 mg) was dispersed into the solution (45 mL) and the suspension was transferred to a reaction cell made of Pyrex glass and was stirred by a magnetic stirrer. After deaeration of the suspension with Ar, UV light was irradiated with a 500 W high-pressure mercury lamp for 5 h. After the photoirradiation, the suspension was filtered, and the obtained powder was dried. The crystal structure of the powder was examined by PXRD measurement.

2.3 Photocatalytic activity measurement

Photocatalytic activity of a catalyst was examined by a gas-closed circulation system equipped with a GC-TCD (Shimadzu, GC-8A). Catalyst sample (0.3-0.5 g) was dispersed into 500 mL of 0.01 M AgF aqueous solution in an inner-irradiation-type reaction cell made of Pyrex glass. The reaction cell was connected to the gas-closed circulation system, and then the suspension was deaerated with stirring by a magnetic stirrer. After the introduction of He gas, UV light was irradiated with a 100 W high-pressure mercury lamp, and the amount of O₂ evolved was quantified by GC. After the reaction, the amount of Ag deposition was quantified by ICP measurement (Seiko Instruments Inc., SPS1700). The

catalyst surface after the photoreaction was examined by means of SEM-EDX observation (Hitach Science Systems, Ltd., SEMEDX TypeN).

3. Results and discussion

3.1 Structural analysis

Table 1 summarizes the synthesis conditions and crystal structures of double perovskites tested in this study. The calcination conditions were optimized to minimize the amount of impurity phases for all the perovskite oxides. For W- and Ti-containing double perovskites, the lattice parameters and the cation arrangements of the ordered double perovskites were consistent with those in the previous reports¹⁰⁻¹³). Rietveld analyses confirmed that these compounds had the rock-salt arrangement of B-cations in the crystal structures.

In this study, we newly synthesized perovskite oxides, LaBaB²⁺B⁷⁵⁺O₆ (B²⁺ = Co, Ni, B⁷⁵⁺ = Ta, Nb) and LaBaZnNbO₆. The characteristic diffraction lines from cubic perovskite-type structure were observed in their PXRD patterns (data are not shown). Concerning the cubic double perovskite, superlattice structure with a unit cell of $2a_p \times 2a_p \times 2a_p$, where a_p is a lattice constant of primitive cubic ABO₃ type perovskite, is formed due to the alternate arrangement of B-cations. Therefore, superlattice diffraction lines appear in the PXRD patterns for these perovskites⁶). The superlattice diffraction lines were clearly observed in the PXRD patterns of the Ta-

and Nb-containing double perovskites, indicating that the rock-salt arrangement of B-cations was also formed in crystal structures of these samples.

3.2 Stability of ordered double perovskite under photocatalytic conditions

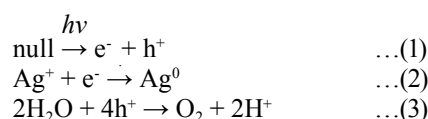
It has been reported that ZnO suffers photocorrosion when it is used in liquid-solid heterogeneous photoreaction¹⁴), in marked contrast with TiO₂ which showed high stability under the various photoreaction conditions. Also, W-oxides easily decomposed to form soluble tungstate species in alkali media. Therefore, it is indispensable to investigate the catalyst stability of the perovskite oxides under the photoreaction conditions. Table 2 shows the stabilities of the W-, Ta-, Nb- and Ti-containing ordered double perovskites in aqueous methanol solution and AgNO₃-containing aqueous solution under photoirradiation. After the photoirradiation in the aqueous methanol solution, A²⁺WO₄ (A²⁺ = Ba, Sr) and the other crystal phases were detected by PXRD measurement for A²⁺₂B²⁺WO₆ (A²⁺ = Ba, Sr, B²⁺ = Cu, Zn), and only the diffraction lines from perovskite phase were observed for A²⁺₂B²⁺WO₆ (A²⁺ = Ba, Sr, B²⁺ = Co, Ni), indicating that Co/W and Ni/W systems were stable and Cu/W and Zn/W systems were unstable under the condition. For A²⁺₂B²⁺WO₆ (A²⁺ = Ba, Sr, B²⁺ = Co, Ni), however, diffraction lines from Ag₂WO₄ (and Ag₂O) in addition to perovskite phase were observed after photoirradiation in the AgNO₃-containing aqueous solution. Thus, these perovskites were decomposed

under the reaction conditions. These findings suggested that W-containing perovskites were not suitable for the photocatalytic reaction in aqueous media because of their low stability.

As for the Ta-, Nb- and Ti-containing ordered double perovskites, on the other hand, no differences in the crystal structures were observed before and after photoirradiation in both of the aqueous solutions, indicating the high stability of the oxides under the conditions without the photocorrosion of Ti and Zn oxides. The results suggested the stability of ordered double perovskite depended strongly on the nature of high valence B-cation.

3.3 Photocatalytic activity of La₂ZnTiO₆

Catalytic test reaction was conducted with the perovskite oxides synthesized in this study, and our study revealed that La₂ZnTiO₆ showed the activity for O₂ evolution from Ag⁺ ion-containing aqueous solution. The reaction mechanism on semiconductor photocatalysts, such as TiO₂ has been well studied and the reaction pathway can be expressed in eqs.(1)-(3).



Here, e⁻, and h⁺ refer to excited electron and hole, respectively. The excited electron reduces Ag⁺ ion to Ag⁰ metal and hole oxidizes water to form O₂.

Table 2 Stability of ordered double perovskite under photoirradiation in methanol and AgNO₃ aqueous solutions ^{a)}

Compound	In a methanol aqueous solution	In an AgNO ₃ aqueous solution
	Stability ^{a)}	Stability ^{a)}
Ba ₂ CoWO ₆	Stable	Ba ₂ CoWO ₆ , Ag ₂ WO ₄
Ba ₂ NiWO ₆	Stable	Ba ₂ NiWO ₆ , Ag ₂ WO ₄ , Ag ₂ O
Ba ₂ CuWO ₆	Ba ₂ CuWO ₆ , BaWO ₄	-
Ba ₂ ZnWO ₆	BaWO ₄ , ZnO	-
Sr ₂ CoWO ₆	Stable	Sr ₂ CoWO ₆ , Ag ₂ WO ₄
Sr ₂ NiWO ₆	Stable	Sr ₂ NiWO ₆ , Ag ₂ WO ₄ , Ag ₂ O
Sr ₂ CuWO ₆	SrWO ₄ , CuO	-
Sr ₂ ZnWO ₆	SrWO ₄ , ZnO	-
LaBaCoTaO ₆	Stable	Stable
LaBaNiTaO ₆	Stable	Stable
LaBaCoNbO ₆	-	Stable
LaBaNiNbO ₆	-	Stable
LaBaZnNbO ₆	-	Stable
La ₂ ZnTiO ₆	Stable	Stable

a) Stability was examined by PXRD patterns before and after photoirradiation in aqueous solutions of methanol and AgNO₃.

Fig. 2 shows the time course for O₂ evolution from a 0.01 M AgF aqueous solution over La₂ZnTiO₆. The amount of O₂ evolved increased with time up to 8 h, and then the O₂ evolution stopped in dark, indicating that the O₂ evolution photocatalytically proceeded over La₂ZnTiO₆. The activity for O₂ evolution over commonly used TiO₂ (P 25) was investigated and compared with that of La₂ZnTiO₆ (Table 3). The total amount of O₂ evolved over La₂ZnTiO₆ was quite lower than that over TiO₂, but the amount of O₂ normalized by catalyst surface area was one third of that of TiO₂.

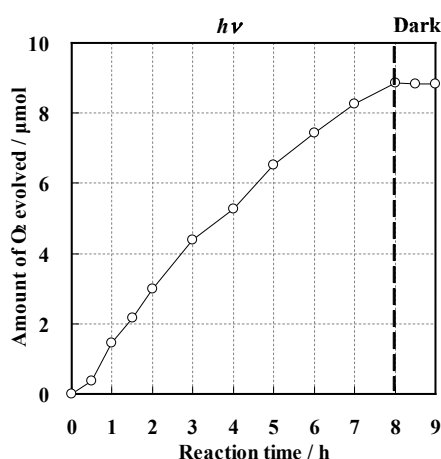


Fig. 2 Time course of O₂ evolution from a 0.01 M AgF aqueous solution over La₂ZnTiO₆ (0.5 g).

PXRD studies confirmed that the reduction of Ag⁺ to Ag⁰ proceeded on La₂ZnTiO₆ catalyst during the photoirradiation in Ag⁺-containing aqueous solution. Fig. 3 shows the PXRD patterns of the catalyst used for the reaction. A characteristic XRD peak for Ag⁰ was observed at 2θ = 38.2 degree. The SEM-EDX observation further provided the evidence for formation of Ag⁰ metal species on the catalyst surface. As shown in Fig. 4, deposition of rod-shape Ag metal over La₂ZnTiO₆ was observed, which further supported that the Ag reduction (eq.(2)) proceeded on the catalyst surface.

Table 3 also summarizes the results for the quantification of Ag metal deposited on La₂ZnTiO₆ after the reaction. According to the stoichiometry in eqs.(1)-(3), the theoretical molar ratio of Ag to O₂ is 4.0. For La₂ZnTiO₆, the ratio of Ag/O₂ showed 5.7 and was deviated from the theoretical value. As for the

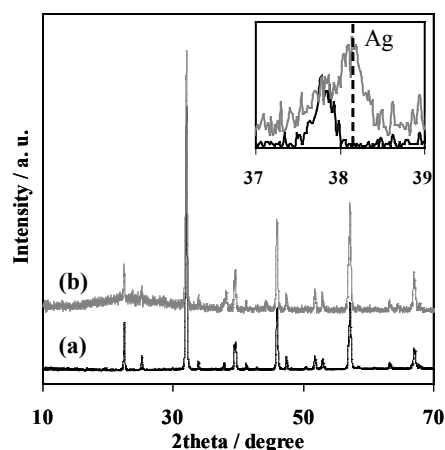


Fig. 3 PXRD patterns of La₂ZnTiO₆ (a) before and (b) after photoirradiation in a 0.02 M AgNO₃ aqueous solution

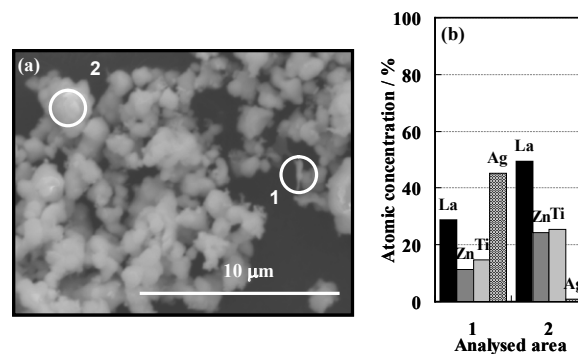


Fig. 4 SEM image (a) and results of the elemental analysis (b) of La₂ZnTiO₆ after photoirradiation in a 0.02 M AgNO₃ aqueous solution.

photocatalytic O₂ evolution over TiO₂ in an AgF aqueous solution, Nishimoto *et al.* has reported that the ratio of Ag/O₂ was larger than 4.0 due to the adsorption of evolved O₂ on the photocatalyst¹⁵⁾. If one considers that O₂ adsorbs on the surface B-cations (Zn²⁺, Ti⁴⁺) in the ratio of 1:1 for La₂ZnTiO₆, the amount of O₂ adsorbed on the catalyst is estimated to be 2.4 μmol assuming 10¹ crystal plane. When this value is taken into account, the ratio of Ag/O₂ is 4.5 and became closer to the theoretical value of 4.0.

Fig. 5 shows the DR UV-VIS spectra of La₂ZnTiO₆ and TiO₂ P25. The absorption edge for La₂ZnTiO₆ was

Table 3 Photocatalytic activity of La₂ZnTiO₆ and TiO₂ for O₂ evolution from a 0.01 M AgF aqueous solution

Sample	Specific surface area / m ² g ⁻¹	O ₂ evolution ^{a)}		Amount of Ag deposited / μmol ^{c)}	Ratio of Ag/O ₂
		μmol ^{b)}	μmol (m ² _{-cat}) ⁻¹		
La ₂ ZnTiO ₆	0.8	8.9	22.3	51	5.7
TiO ₂	55.3	1153.8	69.5	-	-

a) 0.5 g of La₂ZnTiO₆ and 0.3 g of TiO₂ were used for the reaction, b) amount of gas evolved after 8 h photoirradiation, c) quantified by ICP measurement.

observed at shorter wavelength than that for TiO_2 . Optical band gap of $\text{La}_2\text{ZnTiO}_6$ was estimated from the spectra by extrapolating the linear portion to x axis, and the gap was 3.9 eV. This value was much larger than that of TiO_2 3.3 eV estimated from the spectrum. TiO_2 (P 25) is well known as the mixture of anatase and rutile phases in the ratio of 80% and 20%, respectively. Therefore, the optical property of TiO_2 (P 25) is governed by that of the major phase, and the gap is close to that of anatase phase (3.2 eV^2). DR UV-VIS spectrum of $\text{La}_2\text{ZnTiO}_6$ suggested the absence of unreacted TiO_2 , because it did not absorb light longer than about 350 nm. This excludes the possibility that impurity TiO_2 acted as the photocatalyst for the reaction and ensures the occurrence of photocatalytic O_2 evolution over $\text{La}_2\text{ZnTiO}_6$. $\text{La}_2\text{ZnTiO}_6$ showed almost no activity for H_2 generation in aqueous methanol solution. This can be ascribed to the lack of H_2 generation sites, such as Pt, Rh, and RuO_x on the surface of $\text{La}_2\text{ZnTiO}_6$ perovskite.

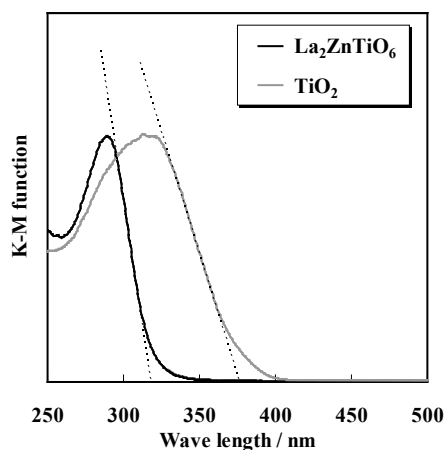


Fig. 5 Absorption spectra of $\text{La}_2\text{ZnTiO}_6$ and TiO_2 .

4. Conclusions

To investigate the applicability of the W-, Ta-, Nb- and Ti-containing ordered double perovskite to photocatalytic reactions, 14 kinds of ordered double perovskites were systematically synthesized and characterized by PXRD measurements. The W-containing ordered double perovskites decomposed under the photoreaction

conditions, photoirradiation in aqueous methanol solution or in Ag^+ ion-containing aqueous solution. On the other hand, Ta-, Nb- and Ti-containing ordered double perovskites were stable under the same conditions, indicating that the stability of ordered double perovskite depended mostly on the nature of high valence B-cation.

Among the perovskite oxides tested in this study, $\text{La}_2\text{ZnTiO}_6$ showed the activity for O_2 evolution and Ag reduction. The reduction of Ag^+ ion to Ag^0 on the surface was confirmed by PXRD and SEM-EDX studies. The activity of $\text{La}_2\text{ZnTiO}_6$ for Ag reduction normalized by the catalyst surface area was one third of that of TiO_2 .

Acknowledgements: This work was partly supported by Grant-in-Aid for Scientific Research on Priority Areas (No. 19028050 and 20037053, ‘‘Chemistry of Concerto Catalysis’’) from Ministry of Education, Culture, Sports, Science and Technology, Japan and a grant from the Global-Centre of Excellence in Novel Carbon Resource Sciences, Kyushu University.

References

- 1) F. E. Osterloh, *Chem. Mater.*, **20**, 35 (2008).
- 2) A. Kudo, Y. Miseki, *Chem. Soc. Rev.*, **38**, 253 (2009).
- 3) H. Kato, H. Kobayashi, A. Kudo, *J. Phys. Chem. B*, **106**, 12441 (2002).
- 4) H. Kato, A. Kudo, *J. Phys. Chem. B*, **105**, 4285 (2001).
- 5) J. Yin, Z. Zou, J. Ye, *J. Phys. Chem. B*, **107**, 61 (2003).
- 6) M. T. Anderson, K. B. Greenwood, G. A. Taylor, K. R. Poeppelmeier, *Prog. Solid St. Chem.*, **22**, 197 (1993).
- 7) G. King, P. M. Woodward, *J. Mater. Chem.*, **20**, 5785 (2010).
- 8) Y. Teraoka, M.-D. Wei, S. Kagawa, *J. Mater. Chem.*, **8**, 2323 (1998).
- 9) F. Izumi, T. Ikeda, *Mater. Sci. Forum*, **198**, 321 (2000).
- 10) E. J. Fresia, L. Katz, R. Ward, *J. Am. Chem. Soc.*, **81**, 4783 (1959).
- 11) D. Iwanaga, Y. Inaguma, M. Itoh, *J. Solid St. Chem.*, **147**, 291 (1999).
- 12) M. Gateshki, J. M. Igartua, E. Hernandez-Bocanegra, *J. Phys. Cond. Matter*, **15**, 6199 (2003).
- 13) R. Uvic, Y. Hu, I. Abrahams, *Acta Cryst.*, **B62**, 521 (2006).
- 14) D. E. Scaife, *Solar Energy*, **25**, 41 (1980).
- 15) S. Nishimoto, B. Ohtani, H. Kajiwara, T. Kagiya, *J. Chem. Soc., Faraday Trans. 1*, **79**, 2685 (1983).